Precision Loss Analysis and Its Solution in Calculation of Electromagnetic Wave Propagation in Reentry Plasma Sheath

Xuyang Chen [1], Fangfang Shen [1], Yanming Liu [1], Wei Ai [2], and Xiaoping Li [1]

[1] School of Aerospace Science and Technology
Xidian University, Xi'an, Shaanxi 710071, China
xychen@mail.xidian.edu.cn, ffshen@mail.xidian.edu.cn, ymliu@xidian.edu.cn, xpli@xidian.edu.cn

[2] Science and Technology on Space Physics Laboratory
China Academy of Launch Vehicle Technology, Beijing 100076, China
27821126@qq.com

Abstract — In this paper, the precision loss problem in calculation of EM wave propagation in the extreme reentry plasma sheath environment is analyzed. Furthermore, we propose a numerical calculation method with controllable precision to deal with this problem. The simulation results show the effect of computational precision loss on EM wave propagation in reentry plasma sheath and also illustrate the validity of the controllable precision calculation method.

Index Terms — Controllable precision, EM wave propagation, numerical calculation, precision loss, reentry plasma sheath.

I. INTRODUCTION

It has generated increasing concern about the interactions of electromagnetic (EM) wave with plasma in recent decade years [1-6], which refers to several applications, such as, analysis of reentry plasma sheath, plasma stealth, nuclear fusion control, etc. The reentry plasma sheath, as a special type of plasma, has several distinct characteristics, such as, extreme electron density and time variation, which severely influence the communication with the reentry object and the radar detection of the object. The extreme parameters (especially for the electron density) will cause precision loss in calculation of EM wave propagation, further causing computational error or even misdirection in EM calculation and simulation. The extreme characteristics mainly occur at the head location of a plasma-covered object. For the electron density, it has reached $10^{19}/m^3$ or even $10^{20}/m^3$ at the head location in a reentry flight [7,8]. However, the researchers [1-3, 9-11] studying the interaction between EM wave and reentry plasma sheath mainly focus on the side or tail locations of the object, where the plasma is far less extreme than that at the head location. Certainly, due to this reason, the computational error in their studies is trivial and can be ignored. Whereas, the plasma influence with extreme parameters (especially for the head location of object) cannot be ignored. This will inevitably give rise to the precision loss problem.

In our previous work [12], we have pointed out that the precision loss problem in calculation of EM wave propagation in plasma sheath lies in the limited numerical calculation precision of computer (usually it is double precision). In this paper, we will give further qualitative and quantitative analysis on the precision loss problem. Then, we propose a computing method with controllable precision based on python platform. By this method, the EM wave propagation in plasma sheath can be computed in a much higher precision by a controllable number of digits, eliminating the precision loss problem. In the simulation, the effect of computational precision loss on EM wave propagation is presented, and the validity of the controllable precision calculation method is illustrated.

The remainder of the paper is organized as follows. Sec. II presents the background of EM wave propagation in plasma. The precision loss analysis and its solution in calculation of EM wave propagation in plasma sheath are shown in Sec. III. Section IV shows the simulation results. The conclusions are finally given in Sec. V.

II. BACKGROUND OF EM WAVE PROPAGATION IN PLASMA

A typical stratification model [4,13] for EM wave propagating in plasma environment is presented in Fig. 1. As can be seen in Fig. 1, an EM plane wave (with its electric part labeled by E_i) is transmitted along x-axis into a nonuniform plasma slab. In each sub-slab (or layer), the plasma is thought to be uniform. The layers are labeled by $l_0, l_1, ..., l_p$ from front-layer (where the EM wave enters into the plasma) to bottom-layer (usually

Submitted On: October 14, 2017
Accepted On: January 22, 2018

corresponding to the metallic surface of an object), respectively. The thickness of layer l_m is represented by $d_{m+1}-d_m$, $m\in\{0,1,2,...,p\}$ (note: d_1=d_0=0), and B denotes the background magnetic field in the plasma environment.

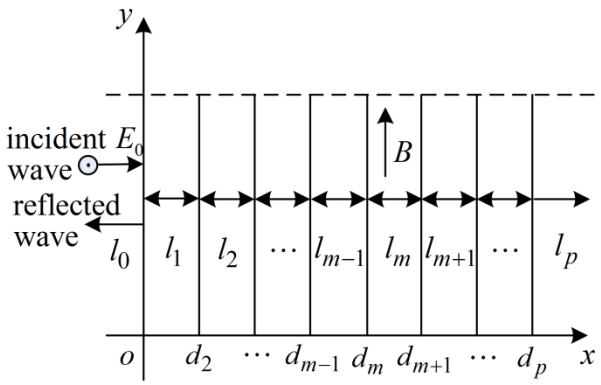

Fig. 1 Stratification model of nonuniform plasma.

The total electric field in layer l_m can be expressed as the following form:

$$E_z^{(m)}(x)=E_0B_m\exp\left(-jk_x^{(m)}(x-d_m)\right)+E_0C_m\exp\left(jk_x^{(m)}(x-d_m)\right),\quad x\in[d_m,d_{m+1}),\tag{1}$$

where E_0 is the input electric field at location x=0, $k_x^{(m)}$ is the complex propagation coefficient in layer l_m, and B_m and C_m are the transmission coefficient and the reflection coefficient at the interface between layers l_{m-1} and l_m, respectively. The detailed expression of $k_x^{(m)}$ can be found in Appendix Section.

There are two important parameters: the total reflection coefficient C_0 and the total transmission coefficient B_p, which reflect the EM reflection and transmission properties of the whole plasma, respectively. These two parameters can be obtained by iteratively solving the equations of boundary conditions [4,14]:

$$\begin{cases} B_m + C_m = B_{m-1}\exp(-jk_x^{(m-1)}(d_m-d_{m-1})) + C_{m-1}\exp(jk_x^{(m-1)}(d_m-d_{m-1})) \\ k_x^{(m)}B_m - k_x^{(m)}C_m = k_x^{(m-1)}B_{m-1}\exp(-jk_x^{(m-1)}(d_m-d_{m-1})) - k_x^{(m-1)}C_{m-1}\exp(jk_x^{(m-1)}(d_m-d_{m-1})) \end{cases},$$
$$m\in\{1,2,...,p\},\tag{2}$$

For conveniently analysis in next section, the Equation (2) is expressed as a matrix form by:

$$\begin{pmatrix}B_m\\C_m\end{pmatrix}=\mathbf{S_m}\begin{pmatrix}B_{m-1}\\C_{m-1}\end{pmatrix},\quad m\in\{1,2,...,p\},\tag{3}$$

where $\mathbf{S_m}$ is called scattering matrix, expressed by:

$$\mathbf{S_m}=\begin{pmatrix}1 & 1\\ k_x^{(m)} & -k_x^{(m)}\end{pmatrix}^{-1}\times\begin{pmatrix}\exp(-jk_x^{(m-1)}(d_m-d_{m-1})) & \exp(jk_x^{(m-1)}(d_m-d_{m-1}))\\ k_x^{(m-1)}\exp(-jk_x^{(m-1)}(d_m-d_{m-1})) & -k_x^{(m-1)}\exp(jk_x^{(m-1)}(d_m-d_{m-1}))\end{pmatrix}.\tag{4}$$

The iterative description of (3) containing the coefficients C_0 and B_p can be expressed by:

$$\begin{pmatrix}B_p\\0\end{pmatrix}=\prod_{m=p}^{1}\mathbf{S_m}\begin{pmatrix}1\\C_0\end{pmatrix}=\mathbf{S_g}\begin{pmatrix}1\\C_0\end{pmatrix},\tag{5}$$

where $\mathbf{S_g}=\prod_{m=p}^{1}\mathbf{S_m}$ is the cascaded scattering matrix. The coefficients C_0 and B_p can then be obtained by solving (5).

III. PRECISION LOSS AND ITS SOLUTION IN CALCULATION OF EM WAVE PROPAGATION IN PLASMA SHEATH

A. Analysis of precision loss

The extreme plasma environment almost always occurs in the reentry flight of a reentry vehicle, especially for the head portion of the vehicle, accompanied by extreme plasma parameters [8]. Among those parameters shown in Sec. II, $k_x^{(m)}$ is a key one, since it is included in the exponent part of the term $\exp(\bullet)$. A larger $|k_x^{(m)}|$ will lead to a much higher rate of increase or decrease of the term $|\exp(\bullet)|$. This will produce a quasi-singular form of the scattering matrix $\mathbf{S_m}$. In detail, it is due to the coexist of the term $\exp(-jk_x^{(m-1)}(d_m-d_{m-1}))$ and its reverse form $\exp(jk_x^{(m-1)}(d_m-d_{m-1}))$ in matrix $\mathbf{S_m}$ as shown in (4). The quasi-singular expression of (4) is adverse to the iterative solution of coefficients and may cause the precision loss. For simplifying description below, let:

$$\xi_{(m-1)}=\exp(jk_x^{(m-1)}(d_m-d_{m-1}))$$
$$\text{and }\xi_{(m-1)}^{-1}=\exp(-jk_x^{(m-1)}(d_m-d_{m-1})).$$

It is not difficult to find that the iterative calculation of (3) and (4) can be divided into the four basic operations: add, subtraction, multiplication, and division. For the case of extreme parameters, the precision loss is possible to occur in the operation of the subtraction of two large quantities with the same sign or approximate argument. Specifically, when the two large numbers are numerically approximate, the precision loss is highly probable to occur. Putting the quasi-singular expression of (4) into consideration, we find that the subtraction operations of two large numbers with numerically approximation occur in a high probability in the iterative calculation of coefficients. It should be noted that the

number of valid digits of a double-precision number (adopted by most computers) is only 16. Whereas, the digits of the term $|\xi_{(m-1)}|$ in (4) may be significantly larger than 16 for the extreme plasma sheath. If this case occurs, the subtraction of two big numbers in calculation of (4) will result in obvious or even huge precision loss. The exact estimation of the digits of $|\xi_{(m-1)}|$, however, is intractable, which relates to a complicated interaction of several parameters as shown in Appendix Section. As an available way, the numerical estimation on digits and on precision loss under selected reasonable parameters will be workable.

Before the presentation of numerical estimation, the computational error of the total reflection coefficient C_0 and that of the total transmission coefficient B_p caused by the precision loss should be analyzed. Based on our analysis, we find that the precision loss is not applied equally to C_0 and B_p, but most of it is applied to B_p. This can be explained by exploring the equation form of (5). For clear description, the Equation (5) is rewritten as the following form:

$$\begin{pmatrix} B_p \\ 0 \end{pmatrix} = \begin{pmatrix} S_{g11} & S_{g12} \\ S_{g21} & S_{g22} \end{pmatrix} \begin{pmatrix} 1 \\ C_0 \end{pmatrix}, \tag{6}$$

where S_{g11}, S_{g12}, S_{g21}, S_{g22} are the four elements of matrix $\mathbf{S_g}$. Suppose we have had the prior knowledge that the elements of $\mathbf{S_g}$ are large numbers. Then, one can find that the solution of C_0 relates to the division of S_{g21} by S_{g22}, which will generate little or trivial precision loss. Whereas, the solution of B_p refers to the add (or subtraction) of two large numbers S_{g11} and $S_{g12}C_0$, which will generate obvious precision loss.

Table 1: Calculated plasma parameters for three selected electron densities

Calculated Parameters	Electron Density n_e (m^{-3})		
	10^{18}	10^{19}	10^{20}
$\lvert\xi_{(1)}\rvert$	1.87×10^{2}	1.24×10^{22}	5.03×10^{74}
C_0	$0.19+0.18j$	$-0.62+0.56j$	$-0.92+0.22j$
B_p	$3.98\times10^{-6}-1.71\times10^{-6}j$	$5.24\times10^{5}j$	$3.14\times10^{57}j$
Abs. Err. of C_0	1.00×10^{-16}	0	3.38×10^{-16}
Abs. Err. of B_p	4.25×10^{-15}	5.24×10^{5}	3.14×10^{57}

To show the precision loss as well as the number of digits in a numerical view, we give an example of the absolute calculation errors for three selected electron densities as shown in Table 1. The main selected constant parameters in Table 1 are shown below: number of layers p=2, plasma thickness d_p=0.1m, collision frequency $f_v = 5\text{GHz}$, incident frequency of EM wave $f = 10\text{GHz}$, material of floor media: titanium alloy with conductivity $\sigma = 2.3\times10^{6}\text{S/m}$.

The calculated parameters $|\xi_{(1)}|$, C_0, and B_p in Table 1 are computed in double precision based on the algorithm in Sec. II. For the true coefficients C_0 and B_p (not the calculated ones in Table 1), they are obtained in an analytic way that is only possible for the ideal plasma case with 2 layers in Table 1 but almost impossible for realistic case. The detailed relation between the electron density n_e and the complex propagation coefficient $k_x^{(m)}$ can be found in Appendix for interested readers.

As shown in Table 1, the calculated parameters for the three electron densities n_e are very different. Only the case for $n_e = 10^{18}/\text{m}^3$ generates no or trivial calculation errors. Whereas, with the increase of n_e, the parameter $|\xi_{(1)}|$ changes quite rapidly and generates large calculation errors. But, coinciding with our analysis, only the calculation of B_p generates large errors but that of C_0 nearly produces no error.

B. Solution of precision loss

The precision loss in the calculation of EM wave propagation can be traced to the shortage of precision in numerical calculation of computer. The commonly used data representation format in most computer systems is double precision with 64-bit. This data format shows limitation when it is used to calculate the EM wave propagation in the extreme environment of reentry plasma sheath. One solution is to increase the numerical calculation precision. There are two ways which can be used to implement it. 1) increasing the float representation bits, such as, 128-bit, 256-bit; 2) converting to integer representation. Considering the complexity and availability, we use the second way.

A matrix calculation technique with controllable precision is put forward here to deal with the precision loss problem. It can be found that the matrix computation procedure shown in Sec. II can be decomposed into the four fundamental arithmetic operations of the elements of the matrixes. To carry out the high-precision calculation, each element of the matrixes is expressed by an integer form (including real part and imaginary part) with fixed digitals. Then, the whole EM wave calculations can be implemented in integer arithmetic operations.

For any a complex element number $\chi = \chi_{real} + j\chi_{imag}$, its integer form can be expressed by:

$$\chi_{\mathrm{INT}} = \lfloor 10^n \chi_{real} \rfloor + j \lfloor 10^n \chi_{imag} \rfloor, \quad (7)$$

where '$\lfloor \cdot \rfloor$' denotes the 'round down' operation, and n is the fixed digital number. The add or subtraction of two numbers $\chi^{(1)}$ and $\chi^{(2)}$ is simple and not shown here. For the multiplication of the two numbers, it is implemented by:

$$\mathrm{mul}(\chi^{(1)}, \chi^{(2)}) \underline{\underline{def}} \frac{\chi^{(1)}_{\mathrm{INT}} \cdot \chi^{(2)}_{\mathrm{INT}}}{10^n}, \quad (8)$$

where '$\mathrm{mul}(\cdot)$' denotes the integer multiplication operation, and $\chi^{(1)}_{\mathrm{INT}}$ and $\chi^{(2)}_{\mathrm{INT}}$ are the integer expressions of the numbers $\chi^{(1)}$ and $\chi^{(2)}$, respectively. The division of the two numbers is implemented by:

$$\mathrm{div}(\chi^{(1)}, \chi^{(2)}) \underline{\underline{def}} \frac{\chi^{(1)}_{\mathrm{INT}} \cdot \chi^{(2)*}_{\mathrm{INT}} \cdot 10^n}{\left|\chi^{(2)}_{\mathrm{INT}}\right|^2}, \quad (9)$$

where '$div(\cdot)$' denotes the integer division of $\chi^{(1)}$ by $\chi^{(2)}$, and $\chi^{(2)*}_{\mathrm{INT}}$ is the conjugation of $\chi^{(2)}_{\mathrm{INT}}$.

Complying with the above operations, one can calculate the total reflection and transmission coefficients C_0 and B_p in a high accuracy. Clearly, the more digitals n is set, the more accuracy in calculation one gains. Here, we suggest this technique is implemented by Python, in which the setting of digital numbers has no limit.

Finally, we talk about the computational complexity of the algorithm. The stratification algorithm shown in Sec. II has the complexity of $O(pN_f)$ (with p: number of layers, and N_f: samples of incident frequency for analysis). When the controllable-precision method is put into consideration, the complexity becomes to be $O(npN_f)$, where n is the digital number.

IV. SIMULATIONS

The EM wave propagation in reentry plasma sheath with extreme parameters is simulated by both the commonly used double precision and the proposed controllable-precision method. The Python (Version 2.7.6) is utilized to implement the calculation with controllable precision. The digit number for controllable-precision calculation is set as n=80 (referring to Table 1). The incident frequency f ranges from 1MHz to 30GHz (creating 50 frequency samples). The collision frequency of plasma is set to be a constant 5GHz. The number of plasma layer is set as p=13.

Figure 2 shows the simulation results of magnitudes of total transmission coefficient B_p. Figure 2 (a) and Fig. 2 (c) are the results calculated by double precision, and Fig. 2 (b) and Fig. 2 (d) are the results calculated by controllable-precision method. In Fig. 2 (a) and Fig. 2 (b), the electron density is set to be $10^{19}/m^3$. In Fig. 2 (c) and Fig. 2 (d), the electron density n_e ranges from $10^{18}/m^3$ to $10^{20}/m^3$, generating 50 samples of n_e. It should be noted that the setting of parameters above is reasonable and complies with the realistic case. The results of total reflection coefficient C_0 are not presented here due to the weaker comparison effect.

It can be found from Fig. 2 (a) that the precision losses or calculation errors by double precision are prevalent for most of the tested incident frequency f (see the error regions), whereas the correct points or regions occupy a small range of f. This wrong result is severe which even gives a misleading wrong trend. Further considering the variation of electron density n_e in Fig. 2 (c), one can find clearly that the precision loss changes toward larger and wider directions with the increase of n_e. Whereas, the controllable-precision method shows accurate results for all the tested incident frequencies f and electron densities n_e as shown in Figs. 2 (b) and (d).

For the time consumption, it is 0.24s for the controllable-precision method (Fig. 2 (b)) and 0.11s for the commonly used double precision case (Fig. 2 (a)) for the 1-D figures. For the 2-D figures, it is 10.91s for the controllable-precision method (Fig. 2 (d)) and 2.67s for the double precision case (Fig. 2 (c)). Based on the complexity analysis in Sec. III-B, the complexity of the algorithm combined by the controllable-precision method is a multiple of that of the original algorithm with double precision. According to the simulation result and theoretical analysis, this multiple is estimated to be in the range 0.02n~0.06n (n is the digital number). Although there is some time-consuming increase of the controllable-precision method, it is acceptable compared to its gain in precision improvement.

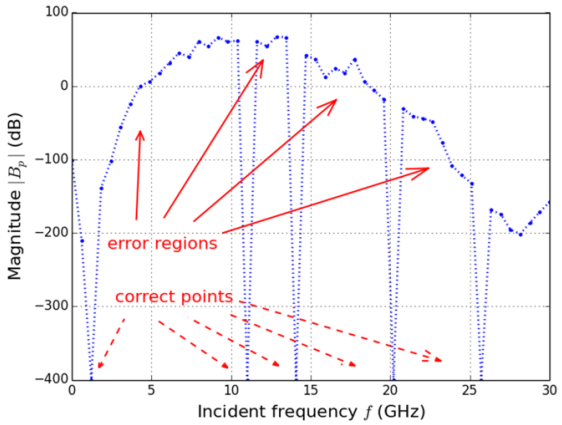

(a)

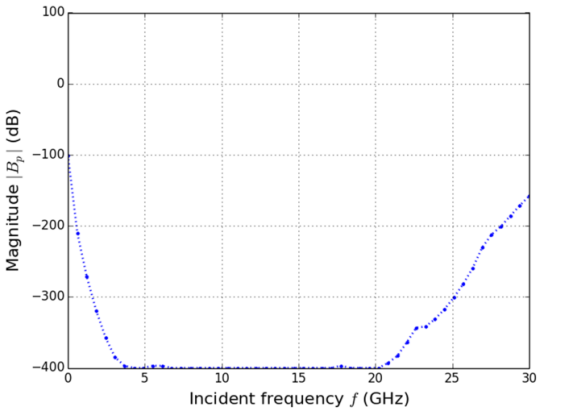

(b)

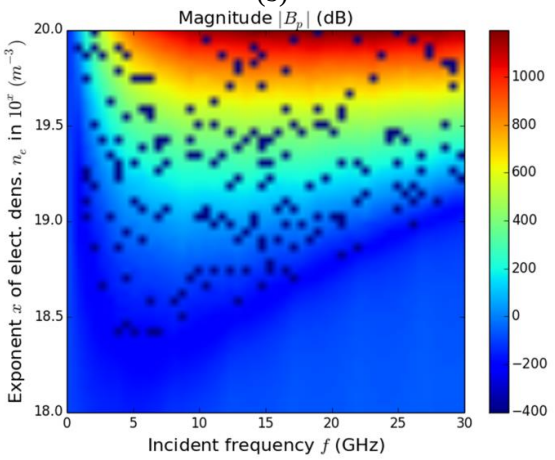

(c)

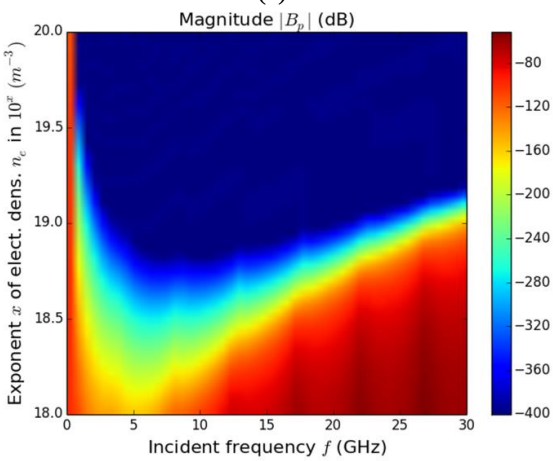

(d)

Fig. 2. Magnitude of transmission coefficient $|B_p|$ calculated by double-precision method and that by controllable-precision method. (a) $|B_p|$ vs. f by double precision with fixing $n_e = 10^{19}/m^3$, (b) $|B_p|$ vs. f by controllable-precision method with fixing $n_e = 10^{19}/m^3$, (c) $|B_p|$ vs. f and n_e by double precision, and (d) $|B_p|$ vs. f and n_e by controllable-precision method.

V. CONCLUSION

The precision loss problem in calculation of EM wave propagating in reentry plasma sheath is analyzed in this paper, and then a solution by numerical calculation with controllable precision is put forward to deal with it. The simulation shows the effect of the precision loss clearly. Also, the proposed controllable-precision calculation method is illustrated to be effective in solving the precision loss problem.

APPENDIX

Relation of propagation coefficient $k_x^{(m)}$, relative complex permittivity $\tilde{\varepsilon}_r^{(m)}$, and electron density n_e [4,15].

The propagation coefficient $k_x^{(m)}$ of the nonuniform plasma in layer l_m is an important parameter related to the EM wave propagation in plasma as described in (1). $k_x^{(m)}$ can be expressed by:

$$k_x^{(m)} = \frac{\omega}{c}\sqrt{\tilde{\varepsilon}_r^{(m)}}, \quad m \in \{0,1,2,...,p\}, \tag{A1}$$

where c is the light speed in vacuum, $\omega = 2\pi f$ is the radian frequency of incident EM wave, and $\tilde{\varepsilon}_r^{(m)}$ is the relative complex permittivity. $\tilde{\varepsilon}_r^{(m)}$ is related to the electric characteristics of a medium. For the plasma medium with layer l_m as shown in Fig. 1, $\tilde{\varepsilon}_r^{(m)}$ can be expressed by:

$$\tilde{\varepsilon}_r^{(m)} = 1 - \frac{\omega_{p,m}^2/\omega^2}{1 - j\frac{\nu_m}{\omega} - \frac{\omega_{ce}^2/\omega^2}{1-\omega_{p,m}^2/\omega^2 - j\nu_m/\omega}}, \quad m \in \{0,1,2,...,p\}, \tag{A2}$$

where $\omega_{p,m}$ and ν_m are the plasma frequency and the collision frequency in m-th layer, respectively, ω_{ce} is the cyclotron frequency of background magnetic field, and all the above symbols are with unit of *rad/s*. The plasma frequency $\omega_{p,m}$ is expressed by:

$$\omega_{p,m} = \sqrt{\frac{n_{e,m}e^2}{\varepsilon_0 m_e}}, \quad m \in \{0,1,2,...,p\}, \tag{A3}$$

where $n_{e,m}$ is the electronic density in plasma layer l_m, ε_0 is the permittivity of vacuum, e and m_e are the electronic quantity and the mass of an electron, respectively.

All the detailed deduction of the above equations (A1~A3) can be found from [15].

ACKNOWLEDGMENT

This work was supported by the National Science Foundation of China under Grants 61701380, the

Science and Technology on Space Physics Laboratory Funds, and the China Postdoctoral Science Foundation (No. 2016M592758).

REFERENCES

[1] K. Xie, M. Yang, B.-W. Bai, X.-P. Li, H. Zhou, and L.-X. Guo, "Re-entry communication through a plasma sheath using standing wave detection and adaptive data rate control," *J. Appl. Phys.*, vol. 119, no. 2, p. 023301, 2016.

[2] S.-H. Liu and L.-X. Guo, "Analyzing the electromagnetic scattering characteristics for 3-D inhomogeneous plasma sheath based on PO method," *IEEE Trans. Plasma Sci.*, vol. 44, no. 11, pp. 2838-2843, Nov. 2016.

[3] M. Yang, X.-P. Li, K. Xie, and Y.-M. Liu, "Parasitic modulation of electromagnetic signals caused by time-varying plasma," *Phys. Plasmas*, vol. 22, no. 2, p. 022120, 2015.

[4] B.-J. Hu, G. Wei, and S.-L. Lai, "SMM analysis of reflection, absorption, and transmission from nonuniform magnetized plasma slab," *IEEE Trans. Plasma Sci.*, vol. 27, no. 4, pp. 1131-1136, Apr. 1999.

[5] H. Torres-Silva, N. Reggiani, and P. H. Sakanaka, "Electromagnetic properties of a chiral-plasma medium," *ACES Journal*, vol. 12, no. 1, pp. 14-18, 1997.

[6] B. T. Nguyen, A. Samimi, and J. J. Simpson, "Recent advances in FDTD modeling of electromagnetic wave propagation in the ionosphere," *ACES Journal*, vol. 29, no. 12, pp. 1003-1012, 2014.

[7] J. P. Rybak and R. J. Churchill, "Progress in reentry communications," *IEEE Trans. Aerosp. Electron. Syst.*, vol. AES-7, no. 5, pp. 879-894, Sept. 1971.

[8] P. W. Huber, N. D. Akey, W. F. Croswell, and C. T. Swift, "The entry plasma sheath and its effects on space vehicle electromagnetic systems," *NASA Tech. Note*, no. SP-252, pp. 1-630, 1971.

[9] S. Liu and S.-Y. Zhong, "Analysis of back-scattering RCS of targets coated with parabolic distribution and time-varying plasma media," *Optik*, vol. 124, no. 24, pp. 6850-6852, 2013.

[10] T. C. Lin and L. K. Sproul, "Influence of reentry turbulent plasma fluctuation on EM wave propagation," *Comput. Fluids*, vol. 35, no. 7, pp. 703-711, 2006.

[11] G.-L. He, Y.-F. Zhan, N. Ge, and Y. Pei, "Measuring the time-varying channel characteristics of the plasma sheath from the reflected signal," *IEEE Trans. Plasma Sci.*, vol. 42, no. 12, pp. 3975-3981, 2014.

[12] X.-Y. Chen, Y.-G. Zhou, Y.-Y. Liu, K.-X. Li, and X.-P. Li, "Precision loss and its solution in calculation of EM wave propagation in plasma environment," in *2017 International Applied Computational Electromagnetics Society Symposium (ACES 2017)*, China: Suzhou, p. 1804, Aug. 2017.

[13] X. Yin, H. Zhang, S.-J. Sun, Z.-W. Zhao, and Y.-L. Hu, "Analysis of propagation and polarization characteristics of electromagnetic waves through nonuniform magnetized plasma slab using propagator matrix method," *Prog. Electromagn. Res.*, vol. 137, no. 1, pp. 159-186, 2013.

[14] W. C. Chew, *Wave and Fields in Inhomogeneous Media*. New York, NY, USA: Van Nostrand Reinhold, 1990.

[15] M. A. Heald and C. B. Wharton, *Plasma Diagnostics with Microwaves*. New York, NY, USA: Krieger, 1978.

Xuyang Chen was born in Hebei, China, in 1980. He received the B.S., M.S., and Ph.D. degrees in Electronic Engineering from Xidian University, Xi'an, China, in 2005, 2008, and 2011, respectively. He joined the CAST-Xi'an Institute of Space Radio Technology, Xi'an, as an Engineer in 2011, where he is involved in radar detection and space navigation. He is currently a Teacher with the School of Aerospace Science and Technology, Xidian University. His current research interests include the radar detection of reentry vehicles covered by plasma sheath.

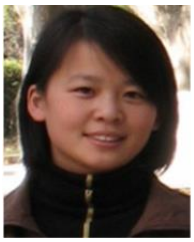

Fangfang Shen received the B.S., M.S. and Ph.D. degrees in Telecommunications Engineering from Xidian University, Xi'an, China, in 2006, 2009, and 2015, respectively. She is currently a Teacher with the School of Aerospace Science and Technology, Xidian University. Her research interests include high-resolution radar imaging and DOA estimation.

Yanming Liu was born in Shaanxi, China, in 1966. He received the B.S., M.S., and Ph.D. degrees from Xidian University, Xi'an, China, in 1989, 1993, and 2003, respectively. He is currently a Full Professor with the School of Aerospace Science and Technology, Xidian University. His current research interests include telecommunication network technology and wireless communication.

Wei Ai was born in Shanxi, China, in 1977. He received the B.S. degree from North University of China in 2000, and M.S. degrees from China Academy of Launch Vehicle Technology in 2011. He is currently a Senior Engineer with China Academy of Launch Vehicle Technology. His current research interests include communication technique and system integration design.

Xiaoping Li was born in Shanxi, China, in 1961. She received the B.S., M.S., and Ph.D. degrees from Xidian University, Xi'an, China, in 1982, 1988, and 2004, respectively. She is currently a Full Professor with the School of Aerospace Science and Technology, Xidian University. Her current research interests include telemetry, tracking and command, and communication technology.